

# RNA-RNA interaction prediction based on multiple sequence alignments

Andrew X. Li<sup>1</sup>, Manja Marz<sup>2</sup>, Jing Qin<sup>3</sup>, Christian M. Reidys<sup>1,4\*</sup>

<sup>1</sup>Center for Combinatorics, LPMC-TJKLC, Nankai University Tianjin 300071, P.R. China

<sup>2</sup>RNA Bioinformatics Group, Philipps-University Marburg, Marbacher Weg 6, 34037 Marburg, Germany

<sup>3</sup>Max Planck Institute for Mathematics in the Sciences, Inselstrasse 22, D-04103 Leipzig, Germany

<sup>4</sup>College of Life Science, Nankai University Tianjin 300071, P.R. China.

Received on \*\*\*\*\*; revised on \*\*\*\*\*; accepted on \*\*\*\*\*

Associate Editor: \*\*\*\*\*

## ABSTRACT

**Motivation** Many computerized methods for RNA-RNA interaction structure prediction have been developed. Recently,  $O(N^6)$  time and  $O(N^4)$  space dynamic programming algorithms have become available that compute the partition function of RNA-RNA interaction complexes. However, few of these methods incorporate the knowledge concerning related sequences, thus relevant evolutionary information is often neglected from the structure determination. Therefore, it is of considerable practical interest to introduce a method taking into consideration both thermodynamic stability and sequence covariation.

**Results** We present the *a priori* folding algorithm *ripalign*, whose input consists of two (given) multiple sequence alignments (MSA). *ripalign* outputs (1) the partition function, (2) base-pairing probabilities, (3) hybrid probabilities and (4) a set of Boltzmann-sampled suboptimal structures consisting of canonical joint structures that are compatible to the alignments. Compared to the single sequence-pair folding algorithm *rip*, *ripalign* requires negligible additional memory resource. Furthermore, we incorporate possible structure constraints as input parameters into our algorithm.

**Availability** The algorithm described here is implemented in C as part of the *rip* package. The supplemental material, source code and input/output files can freely be downloaded from <http://www.combinatorics.cn/cbpc/ripalign.html>.

**Contact** Christian Reidys [duck@santafe.edu](mailto:duck@santafe.edu)

**Keywords** multiple sequence alignment, RNA-RNA interaction, joint structure, dynamic programming, partition function, base pairing probability, hybrid, loop, RNA secondary structure.

## 1 INTRODUCTION

RNA-RNA interactions play a major role at many different levels of the cellular metabolism such as plasmid replication control, viral encapsidation, or transcriptional and translational regulation. With the discovery that a large number of transcripts

in higher eukaryotes are noncoding RNAs, RNA-RNA interactions in cellular metabolism are gaining in prominence. Typical examples of interactions involving two RNA molecules are snRNAs (Forne *et al.*, 1996); snoRNAs with their targets (Bachellerie *et al.*, 2002); micro-RNAs from the RNAi pathway with their mRNA target (Ambros, 2004; Murchison and Hannon, 2004); sRNAs from *Escherichia coli* (Hershberg *et al.*, 2003; Repoila *et al.*, 2003); and sRNA loop-loop interactions (Brunel *et al.*, 2003). The common feature in many ncRNA classes, especially prokaryotic small RNAs, is the formation of RNA-RNA interaction structures that are much more complex than the simple sense-antisense interactions.

As it is the case for the general RNA folding problem with unrestricted pseudoknots (Akutsu, 2000), the RNA-RNA interaction problem (RIP) is NP-complete in its most general form (Alkan *et al.*, 2006; Mneimneh, 2009). However, polynomial-time algorithms can be derived by restricting the space of allowed configurations in ways that are similar to pseudoknot folding algorithms (Rivas and Eddy, 1999). The simplest approach concatenates the two interacting sequences and subsequently employs a slightly modified standard secondary structure folding algorithm. The algorithms RNACofold (Hofacker *et al.*, 1994; Bernhart *et al.*, 2006), pairfold (Andronescu *et al.*, 2005), and NUPACK (Ren *et al.*, 2005) subscribe to this strategy. A major shortcoming of this approach is that it cannot predict important motifs such as kissing-hairpin loops. The paradigm of concatenation has also been generalized to the pseudoknot folding algorithm of Rivas and Eddy (1999). The resulting model, however, still does not generate all relevant interaction structures (Chitsaz *et al.*, 2009b). An alternative line of thought is to neglect all internal base-pairings in either strand and to compute the minimum free energy (MFE) secondary structure for their hybridization under this constraint. For instance, RNAduplex and RNAhybrid (Rehmsmeier *et al.*, 2004) follows this line of thought. RNAup (Mückstein *et al.*, 2006, 2008) and intaRNA (Busch *et al.*, 2008) restrict interactions to a single interval that remains unpaired in the secondary structure for each partner. These models have proved particularly useful for bacterial sRNA/mRNA interactions (Geissmann and Touati, 2004).

Pervouchine (2004) and Alkan *et al.* (2006) independently proposed MFE folding algorithms for predicting the *joint structure* of two interacting RNA molecules with polynomial time

\*to whom correspondence should be addressed. Phone: \*86-22-2350-6800; Fax: \*86-22-2350-9272; [duck@santafe.edu](mailto:duck@santafe.edu)

complexity. In their model, a “joint structure” means that the intramolecular structures of each molecule are pseudoknot-free, the intermolecular binding pairs are noncrossing and there exist no so-called “zig-zags”, see supplement material (SM) for detailed definition. The optimal joint structure is computed in  $O(N^6)$  time and  $O(N^4)$  space via a dynamic programming (DP) routine.

A more reliable approach is to consider the partition function, which by construction integrates over the Boltzmann-weighted probability space, allowing for the derivation of thermodynamic quantities, like e.g. equilibrium concentration, melting temperature and base-pairing probabilities. The partition function of joint structures was independently derived by Chitsaz *et al.* (2009b) and Huang *et al.* (2009) while the base-pairing probabilities are due to Huang *et al.* (2009).

A key quantity here is the probability of hybrids, which cannot be recovered from base pairing probabilities since the latter can be highly correlated. Huang *et al.* (2010) presented a new hybrid-based decomposition grammar, facilitating the computation of the nontrivial hybrid-probabilities as well as the Boltzmann sampling of RNA-RNA interaction structures. The partition function of joint structures can be computed in  $O(N^6)$  time and  $O(N^4)$  space and current implementations require very large computational resources. Salari *et al.* (2009) recently achieved a substantial speed-up making use of the observation that the external interactions mostly occur between pairs of unpaired regions of single structures. Chitsaz *et al.* (2009a) introduced tree-structured Markov Random Fields to approximate the joint probability distribution of multiple ( $\geq 3$ ) contact regions.

Unfortunately, incompleteness of the underlying energy model, in particular for hybrid- and kissing-loops, may result in prediction inaccuracy. One way of improving this situation is to involve phylogenetic information of multiple sequence alignments (MSA).

In an MSA homologous nucleotides are grouped in columns, where homologous is interpreted in *both*: structural as well as evolutionary sense. I.e. a column of nucleotides occupies similar structural positions and all diverge from a common ancestral nucleotide. Also, many ncRNAs show clear signs of undergoing compensatory mutations along evolutionary trajectories. In conclusion, it seems reasonable to stipulate that a non-negligible part of the existing RNA-RNA interactions contain preserved but covarying patterns of the interactions (Seemann *et al.*, 2010). Therefore we can associate a consensus interaction structure to pairs of interacting MSAs (see Section 2.1).

Along these lines Seemann *et al.* (2010) presented an algorithm PETcOfold for prediction of RNA-RNA interactions including pseudoknots in given MSAs. Their algorithm is an extension of PETfold (Seemann *et al.*, 2008) using elements of RNAcofold (Bernhart *et al.*, 2006) and computational strategies for hierarchical folding (Gaspin and Westhof, 1995; Jabbari *et al.*, 2007). However, PETcOfold is an approximation algorithm and further differences between the two approaches will be discussed in Section ??.

Here, we present the algorithm ripalign which computes the partition function, base-pairing as well as hybrid probabilities and performs Boltzmann-sampling on the level of MSAs. ripalign represents a generalization of rip to pairs of interacting MSAs and a new grammar of canonical interaction structures. The latter is of relevance since there are no isolated base pairs in molecular complexes.

sp.	$\bar{\mathbf{R}}$	sp.	$\bar{\mathbf{S}}$	sp.	$\mathbf{R}$	$\mathbf{S}$
$\theta_1$	AGAACGGA	$\theta_1$	GGGCCG	$\theta_1$	AGAACGGA	GGGCCG
$\theta_1$	GAAACGGA	$\theta_1$	AGUUAG	$\theta_1$	AGAACGGA	AGUUAG
$\theta_2$	AGA.CGAC	$\theta_2$	AGGCAG	$\theta_1$	GAAACGGA	GGGCCG
		$\theta_2$	. . GUGG	$\theta_1$	GAAACGGA	AGUUAG
				$\theta_2$	AGA.CGAC	AGGCAG
				$\theta_2$	AGA.CGAC	. . GUGG

**Table 1. Preprocessing in ripalign:** Given a pair of MSAs ( $\bar{\mathbf{R}}, \bar{\mathbf{S}}$ ), where  $\bar{\mathbf{R}}$  consists of three aligned RNA sequences of species (sp.)  $\theta_1$  or  $\theta_2$ .  $\bar{\mathbf{S}}$  in turn consists of four aligned sequences of species  $\theta_1$  and  $\theta_2$ . Then we obtain the matrix-pair  $(\mathbf{R}, \mathbf{S})$ , where  $(\mathbf{R}^i, \mathbf{S}^i)$ ,  $1 \leq i \leq 6$ , ranges over all the six potentially interacting RNA-pairs.

One important step consists in identifying the notion of a joint structure compatible to a pair of interacting MSAs. Our notion is based on the framework of Hofacker *et al.* (2002), where a sophisticated cost function capturing thermodynamic stability as well as sequence covariation is employed. Furthermore ripalign is tailored to take structure constraints, such as blocked nucleotides known e.g. from chemical probing, into account.

## 2 THEORY

### 2.1 Multiple sequence alignments and compatibility

A MSA,  $\bar{\mathbf{R}}$ , consists of  $m_{\bar{\mathbf{R}}}$  RNA sequences of known species. Denoting the length of the aligned sequences by  $N$ ,  $\bar{\mathbf{R}}$  constitutes a  $m_{\bar{\mathbf{R}}} \times N$  matrix, having  $5' - 3'$  oriented rows,  $\mathbf{R}^i$  and columns,  $\bar{\mathbf{R}}_i$ . Its  $(i, j)$ -th entry,  $\bar{\mathbf{R}}_i^j$ , is a nucleotide, **A**, **U**, **G**, **C** or a gap denoted by . .

For any pair  $(\bar{\mathbf{R}}, \bar{\mathbf{S}})$  we assume that  $\bar{\mathbf{S}}$  is a  $m_{\bar{\mathbf{S}}} \times M$  matrix, whose rows carry  $3' - 5'$  orientation.

In the following we shall assume that a pair of RNA sequences can only interact if they belong to the same species. A pair  $(\bar{\mathbf{R}}, \bar{\mathbf{S}})$ , can interact if for any row  $\mathbf{R}^i$ , there exist at least one row in  $\bar{\mathbf{S}}$  that can interact with  $\mathbf{R}^i$ .

Given a pair of interacting MSAs  $(\bar{\mathbf{R}}, \bar{\mathbf{S}})$ , let  $m$  be the total number of potentially interacting pairs. ripalign exhibits a pre-processing step which generates a  $m \times N$ -matrix  $\mathbf{R}$  and a  $m \times M$ -matrix  $\mathbf{S}$  such that  $(\mathbf{R}^i, \mathbf{S}^i)$  range over all  $m$  potentially interacting RNA-pairs, see Tab. 1 and the SM, Section 1.2.

We shall refer in the following to  $\mathbf{R}$  and  $\mathbf{S}$  as MSAs ignoring the fact that they have multiple sequences.

We proceed by defining joint structures that are compatible to a fixed  $(\mathbf{R}, \mathbf{S})$ . To this end, let us briefly review some concepts introduced in Huang *et al.* (2009).

A joint structure  $J(R, S, I)$  is a graph consisting of

- (j1) Two secondary structures  $R$  and  $S$ , whose backbones are drawn as horizontal lines on top of each other and whose arcs are drawn in the upper and lower halfplane, respectively. We consider  $R$  over a  $5'$  to  $3'$  oriented backbone  $(R_1, \dots, R_N)$  and  $S$  over a  $3'$  to  $5'$  oriented backbone  $(S_1, \dots, S_M)$  and refer to any  $R$ - and  $S$ -arcs as interior arcs.
- (j2) An additional set  $I$ , of noncrossing arcs of the form  $R_i S_j$  (exterior arc), where  $R_i$  and  $S_j$  are unpaired in  $R$  and  $S$ .
- (j3)  $J(R, S, I)$  contains no “zig-zags” (see SM).

The subgraph of a joint structure  $J(R, S, I)$  induced by a pair of subsequences  $(R_i, R_{i+1}, \dots, R_j)$  and  $(S_h, S_{h+1}, \dots, S_\ell)$  is denoted by  $J_{i,j;h,\ell}$ . In particular,  $J(R, S, I) = J_{1,N;1,M}$  and  $J_{i,j;h,\ell} \subset J_{a,b;c,d}$  if and only if  $J_{i,j;h,\ell}$  is a subgraph of  $J_{a,b;c,d}$  induced by  $(R_i, \dots, R_j)$  and  $(S_h, \dots, S_\ell)$ . In particular, we use  $S[i, j]$  to denote the subgraph of  $J_{1,N;1,M}$  induced by  $(S_i, S_{i+1}, \dots, S_j)$ , where  $S[i, i] = S_i$  and  $S[i, i-1] = \emptyset$ .

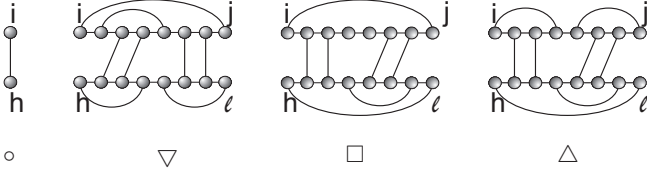


**Fig. 1.** The four basic types of tight structures are given as follows:  $\circ$  :  $\{R_i S_h\} = J_{i,j;h,\ell}$  and  $i = j, h = \ell$ ;  $\nabla$  :  $R_i R_j \in J_{i,j;h,\ell}$  and  $S_h S_\ell \notin J_{i,j;h,\ell}$ ;  $\square$  :  $\{R_i R_j, S_h S_\ell\} \in J_{i,j;h,\ell}$ ;  $\triangle$  :  $S_h S_\ell \in J_{i,j;h,\ell}$  and  $R_i R_j \notin J_{i,j;h,\ell}$ .

Given a joint structure,  $J_{a,b;c,d}$ , a tight structure (TS),  $J_{i,j;h,\ell}$ , (Huang *et al.*, 2009) is a specific subgraph of  $J_{a,b;c,d}$  indexed by its type  $\in \{\circ, \nabla, \square, \triangle\}$ , see Fig. 1. For instance, we use  $J_{i,j;h,\ell}^{\square}$  to denote a TS of type  $\square$ .

A *hybrid* is a joint structure  $J_{i_1,i_\ell;j_1,j_\ell}^{\text{Hy}}$ , i.e. a maximal sequence of intermolecular interior loops consisting of a set of exterior arcs  $(R_{i_1} S_{j_1}, \dots, R_{i_\ell} S_{j_\ell})$  where  $R_{i_h} S_{j_h}$  is nested within  $R_{i_{h+1}} S_{j_{h+1}}$  and where the internal segments  $R[i_h + 1, i_{h+1} - 1]$  and  $S[j_h + 1, j_{h+1} - 1]$  consist of single-stranded nucleotides only. That is, a hybrid is the maximal unbranched stem-loop formed by external arcs.

A joint structure  $J(\mathbf{R}, S, I)$  is called *canonical* if and only if:

(c1) each stack in the secondary structures  $R$  and  $S$  is of size at least two, i.e. there exist no isolated interior arcs,

(c2) each hybrid contains at least two exterior arcs.

In the following, we always assume a joint structure to be canonical.

Next, we come to  $(\mathbf{R}, \mathbf{S})$ -compatible joint structures. In difference to single sequence compatibility, this notion involves statistical information of the MSAs.

The key point consists in specifying under which conditions two vertices contained in  $(R_1, \dots, R_N, S_1, \dots, S_M)$  can pair. This is obtained by a generalization of the RNAalifold approach (Hofacker *et al.*, 2002). We specify these conditions for interior  $(c_{i,j}^{\mathbf{R}}, c_{i,j}^{\mathbf{S}})$  and exterior pairs  $(c_{i,j}^{\mathbf{R},\mathbf{S}})$  in eq. (2.3)-(2.5).

For interior arcs  $(R_i, R_j)$ , let  $X, Y \in \{\mathbf{A}, \mathbf{U}, \mathbf{G}, \mathbf{C}\}$ . Let  $f_{ij}^{\mathbf{R}}(XY)$  be the frequency of  $(X, Y)$  which exists in the 2-column sub-matrix  $(\mathbf{R}_i, \mathbf{R}_j)$  as a row-vector and

$$c_{i,j}^{\mathbf{R}} = \sum_{XY, X'Y'} f_{ij}^{\mathbf{R}}(XY) D_{XY, X'Y'}^{\mathbf{R}} f_{ij}^{\mathbf{R}}(X'Y'). \quad (2.1)$$

Here  $XY$  and  $X'Y'$  independently range over all 16 elements of  $\{\mathbf{A}, \mathbf{U}, \mathbf{G}, \mathbf{C}\} \times \{\mathbf{A}, \mathbf{U}, \mathbf{G}, \mathbf{C}\}$  and  $D_{XY, X'Y'}^{\mathbf{R}} = d_H(XY, X'Y')$ , i.e. the Hamming distance between  $XY$  and  $X'Y'$  in case of  $XY$  and  $X'Y'$  being Watson-Crick, or **GU** wobble base pair and 0, otherwise. Furthermore, we introduce  $q_{i,j}^{\mathbf{R}}$  to deal with the inconsistent sequences

$$q_{i,j}^{\mathbf{R}} = 1 - \frac{1}{m} \sum_h \{\Pi_{i,j}^h(\mathbf{R}) + \delta(\mathbf{R}_i^h, \text{gap})\delta(\mathbf{R}_j^h, \text{gap})\}, \quad (2.2)$$

where  $\delta(x, y)$  is the Kronecker delta and  $\Pi_{i,j}^h(\mathbf{R})$  is equal to 1 if  $\mathbf{R}_i^h$  and  $\mathbf{R}_j^h$  are Watson-Crick or **GU** wobble base pair and 0, otherwise. Now we obtain  $B_{i,j}^{\mathbf{R}} = c_{i,j}^{\mathbf{R}} - \phi_1 q_{i,j}^{\mathbf{R}}$ . Based on sequence data, the threshold for pairing  $B_{i,j}^{\mathbf{R}}$  as well as the weight of inconsistent sequences  $\phi_1$  are computed we have

$$(c_{i,j}^{\mathbf{R}}) \quad B_{i,j}^{\mathbf{R}} \geq B_{i,j}^{\mathbf{R}*} \quad (2.3)$$

The case of two positions  $S_i$  and  $S_j$  is completely analogous

$$(c_{i,j}^{\mathbf{S}}) \quad B_{i,j}^{\mathbf{S}} \geq B_{i,j}^{\mathbf{S}*}, \quad (2.4)$$

where  $B_{i,j}^{\mathbf{S}}$  and  $B_{i,j}^{\mathbf{S}*}$  are analogously defined.

As for  $(c_{i,j}^{\mathbf{R},\mathbf{S}})$  a further observation factors in: since many ncRNA show clear signs of undergoing compensatory mutations in the course of evolution

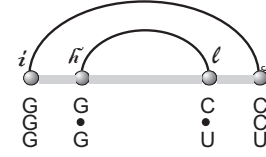


**Fig. 2. Interior loop energy:** An interior loop formed by  $R_i R_j$  and  $R_h R_\ell$ , where  $i < h < \ell < j$  are the alignment positions. Grey bands are used to denote the positions we omit between segment  $(i, h)$ ,  $(h, \ell)$  and  $(\ell, j)$ .

(Seemann *et al.*, 2010; Marz *et al.*, 2008), we postulate the existence of a non-negligible amount of RNA-RNA interactions containing conserved pairs, consistent mutations, compensatory mutations as well as inconsistent mutations. Based on this observation we arrive at

$$(c_{i,j}^{\mathbf{R},\mathbf{S}}) \quad B_{i,j}^{\mathbf{R},\mathbf{S}} \geq B_{i,j}^{\mathbf{R},\mathbf{S}*}, \quad (2.5)$$

where  $B_{i,j}^{\mathbf{R},\mathbf{S}}$  and  $B_{i,j}^{\mathbf{R},\mathbf{S}*}$  are analogously defined as the case for  $B_{i,j}^{\mathbf{R}}$  and  $B_{i,j}^{\mathbf{S}}$ .

A joint structure  $J$  is compatible to  $(\mathbf{R}, \mathbf{S})$  if for any  $J$ -arc, the corresponding intra- or inter-positions can according to eq. (2.3)-(2.5) pair.

## 2.2 Energy model

According to Huang *et al.* (2009) joint structures can be decomposed into disjoint loops. These loop-types include standard hairpin-, bulge-, interior- and multi-loops found in RNA secondary structures as well as *hybrid* and *kissing-loops*. Following the energy parameter rules of Mathews *et al.* (1999), the energy of each loop can be obtained as a sum of the energies associated with non-terminal symbols, i.e. graph properties (sequence independent) and an additional contributions which depend uniquely on the terminal bases (sequence dependent).

Suppose we are given a joint structure  $J$ , compatible to a pair  $\mathcal{P} = (\mathbf{R}, \mathbf{S})$ . Let  $L \in J$  be a loop and let  $\mathcal{F}_{L,i}$  represent the loop energy of the  $i$ -th interaction-pair  $(\mathbf{R}^i, \mathbf{S}^i)$ . Then the loop energy of  $\mathcal{P}$  is

$$\mathcal{F}_{L,\mathcal{P}} = 1/m \sum_i \mathcal{F}_{L,i}. \quad (2.6)$$

We consider the energy of the structure as the sum of all loop contributions:

$$\mathcal{F}_J = \sum_{L \in J} \mathcal{F}_{L,\mathcal{P}}. \quad (2.7)$$

To save computational resources, gaps are treated as bases in `ripalign`. Thus only alignment positions contribute as indices and loop sizes. Since no measured energy parameters for nonstandard base-pairs are available at present time, additional terminal-dependent contributions for the latter are ignored. For instance, let  $\text{Int}_{i,j;h,\ell}$  denote an interior loop formed by  $R_i R_j$  and  $R_h R_\ell$  and  $\mathcal{F}_{\text{Int},\mathcal{P}}^{i,j;h,\ell}$  denote the free energy of  $\text{Int}_{i,j;h,\ell}$  with respect to the aligned sequences in  $\mathcal{P}$ . Then  $\mathcal{F}_{\text{Int},\mathcal{P}}^{i,j;h,\ell}$  associated to the three aligned subsequences of Fig. 2 reads

$$\mathcal{F}_{i,j;h,\ell}^{\text{Int},\mathcal{P}} = \frac{1}{3} (3G_{i,j;h,\ell}^{\text{Int}} + G_{*,\mathbf{G},\mathbf{C};\mathbf{G},\mathbf{C}}^{\text{Int}} + G_{*,\mathbf{G},\mathbf{U};\mathbf{G},\mathbf{U}}^{\text{Int}} + G_{*,\mathbf{G},\mathbf{C};\text{gap,gap}}^{\text{Int}}). \quad (2.8)$$

Here  $G_{i,j;h,\ell}^{\text{Int}}$  represents contributions related exclusively to the positions of the interior loop while  $G_{*,\mathbf{A},\mathbf{B};\mathbf{C},\mathbf{D}}^{\text{Int}}$  represents additional contributions related to the specific nucleotides which form the interior loop. We set  $G_{*,\mathbf{G},\mathbf{C};\text{gap,gap}}^{\text{Int}}$  to be zero.

## 2.3 The grammar of canonical joint structures and the partition function

The partition function algorithm is easily extended to work with the modified energy functions given in eq. (2.7). The reformulation of the original hybrid-grammar into a grammar of canonical joint structures represents already for

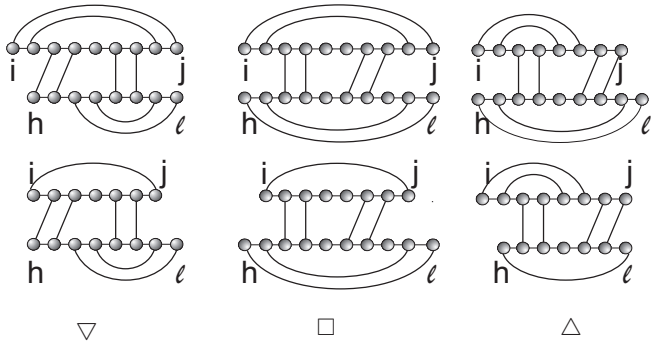


**Fig. 3. Examples of two TS-types.** We display  $\nabla$ ,  $\square$ , or  $\triangle$ -tight structures: Type cc (top) and Type c (bottom).

single interaction pairs a significant improvement in prediction quality. The original rip-grammar would oftentimes encounter joint structures having a hybrid composed by a single isolated exterior arc, see Fig. 8.

In order to decompose canonical joint structures via the unambiguous grammar introduced in Section 2.3, we distinguish the two types (Type cc and Type c) of TS's of type  $\nabla$ ,  $\triangle$  or  $\square$ . Given a TS of type  $\nabla$ , denoted by  $J_{i,j;h,\ell}^{\nabla}$ , we write depending on whether  $R_{i+1}R_{j-1} \in J_{i,j;h,\ell}^{\nabla}$ ,  $J_{i,j;h,\ell}^{\nabla,cc}$  and  $J_{i,j;h,\ell}^{\nabla,c}$ , respectively. Analogously, we define  $J_{i,j;h,\ell}^{\square,cc}$ ,  $J_{i,j;h,\ell}^{\square,c}$  and  $J_{i,j;h,\ell}^{\triangle,cc}$ ,  $J_{i,j;h,\ell}^{\triangle,c}$ , see Fig. 3.

Fig. 4 summarizes the two basic steps of the canonical-grammar: (I) interior arc-removal to reduce TS, and (II) block-decomposition to split a joint structure into two smaller blocks. The key feature here is, that since  $J$  is canonical, the smaller blocks are still canonical after block-decomposition. Each decomposition step displayed in Fig. 4 results in substructures which eventually break down into generalized loops whose energies can be directly computed. More details of the decomposition procedures are described in Section 2 of the SM, where we prove that for any canonical joint structure  $J$ , there exists a unique decomposition-tree (parse-tree), denoted by  $T_J$ , see Fig. 5.

## 2.4 Probabilities and the Boltzmann Sampling

A dynamic programming scheme for the computation of a partition function implies a corresponding computation of probabilities of specific substructures is obtained “from the outside to the inside” and a stochastic backtracing procedure that can be used to sample from the associated distribution (McCaskill, 1990; Ding and Lawrence, 2003; Huang *et al.*, 2010). We remark that the time complexity does not increase linearly as a function of  $m$  (see SM Table. 5).

Along the lines of the design of the Vienna software package (Hofacker *et al.*, 1994), ripalign now offers the following features as optional input parameters:

- (1) a position  $i$  can be restricted to form an interior or an exterior arc. (denoted by “-” and “^”, respectively);
- (2) a position  $i$  can be forced to be unpaired (denoted by “x”);
- (3) a position  $i$  can be restricted to form an (interior or an exterior) arc with some position  $j$  (denoted by “\*”);
- (4) a pair of positions  $i$  and  $j$  can be forced to form an interior or exterior arc (denoted by “()” or “[ ]”, respectively).

However, the above features are optional. Thus ripalign can deal with both scenarios: the absence of any *a priori* information and the existence of specific information, e.g the location of the Sm-binding site, see Fig. 8.

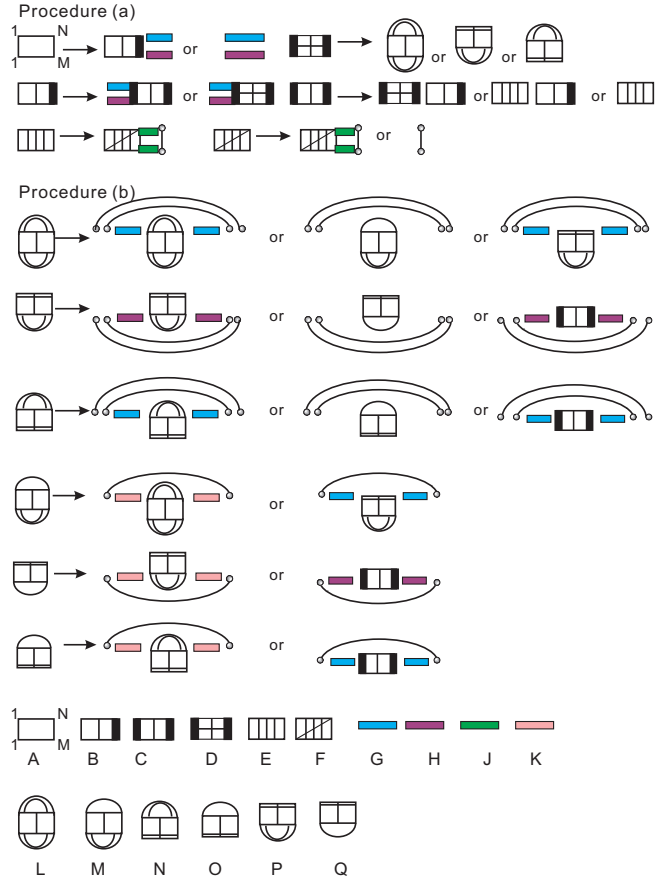


**Fig. 4. Grammar:** Illustration of the decomposition of  $J_{1,N;1,M}$ , DTS, RTS and hybrids in Procedure (a) and of tight structures in Procedure (b). In the bottom row the symbols for the 16 distinct types of structural components are listed: **A:** arbitrary joint structure  $J_{1,N;1,M}$  (canonical); **B:** right-tight structures  $J_{i,j;r,s}^{RT}$ ; **C:** double-tight structure  $J_{i,j;r,s}^{DT}$ ; **D:** tight structure  $J_{i,j;h,\ell}^{\nabla,cc}$ ,  $J_{i,j;h,\ell}^{\triangle,cc}$  or  $J_{i,j;h,\ell}^{\square,cc}$ ; **E:** hybrid structure  $J_{i,j;h,\ell}^{Hy}$ ; **F:** substructure of a hybrid  $J_{i,j;h,\ell}^h$  such that  $R_i S_j$  and  $R_h S_\ell$  are exterior arcs and  $J_{i,j;h,\ell}^h$  itself is not a hybrid since it is not maximal; **G, H:** maximal secondary structure segments  $R[i, j]$ ,  $S[r, s]$ ; **J:** isolated segment  $R[i, j]$  or  $S[h, \ell]$ ; **K:** maximal secondary structure segments appear in pairs such that at least one of them is not empty. **L:** tight structure  $J_{i,j;r,s}^{\square,cc}$ ; **M:** tight structure  $J_{i,j;r,s}^{\square,c}$ ; **N:** tight structure  $J_{i,j;r,s}^{\nabla,cc}$ ; **O:** tight structure  $J_{i,j;r,s}^{\nabla,c}$ ; **P:** tight structure  $J_{i,j;r,s}^{\triangle,cc}$ ; **Q:** tight structure  $J_{i,j;r,s}^{\triangle,c}$ .

## 3 RESULTS AND DISCUSSION

In this paper we present an *a priori*  $O(N^6)$  time and  $O(N^4)$  space dynamic programming algorithm ripalign, whose input consists of a pair of interacting MSAs. ripalign requires only marginally more computational resources but is, without doubt, still computationally costly. Approximation algorithms are much faster, for instance PETCOFOLD (Seemann *et al.*, 2010), having a time complexity of  $O(m(N+M)^3n)$ , where  $m$  is the number of sequences in MSA,  $N$  and  $M$  being the sequence lengths of the longer and shorter alignment, respectively, and  $n < N/2$  is the number of iterations for the adaption of the threshold value to find likely partial secondary structures. Their basic assumption is that the two secondary structures fold independently and that intra-loop evaluation differences are negligible. The flip-side of reducing the complexity of a folding problem by

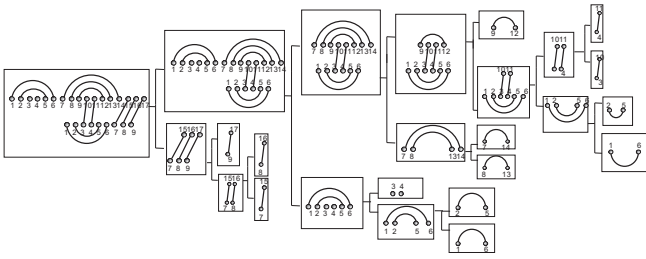


**Fig. 5. Example of the parse tree.** The parse tree of the canonical joint structure  $J_{1,17;1,9}$ .

introducing additional assumptions, is however, the uncertainty of the quality of the solution. Point in case here is that the two secondary structures did not evolve independently, but rather correlated by means of their functional interaction. We remark that `ripalign` (within its complexity limitations) is capable to describe the space of RNA interaction structures, for instance via Boltzmann sampling, in detail and transparency.

`ripalign` represents significant improvements in the following aspects:

- (a) we incorporate evolutionary factors into the RNA-RNA interaction structure prediction via alignments as input,
- (b) we introduce the grammar of canonical joint structures of interacting-alignments,
- (c) we a *a priori* factor in structural-constraints, like for instance, knowledge on Sm-binding sites.

Below we shall discuss (a), (b) and (c) in more detail in the context of concrete examples. All the MSAs involving in (a), (b) and (c) are listed in SM, Section 2.

#### (a): The *fhIA/OxyS* interaction

The *OxyS* RNA represses *fhIA* mRNA translation initiation through base-pairing with two short sequences Argaman and Altuvia (2000), one of which overlaps the ribosome binding sequence and the other resides further downstream, within the coding region of *fhIA*. Our algorithm predicts correctly both interaction sites based on MSAs, see Fig. 6. In addition, most predicted stacks in the secondary structures of *fhIA* and *OxyS* agree well with the most frequent Boltzmann sampled structure. Two more hybrids,  $J_{56,59;41,44}^{\text{Hy}}$  and  $J_{81,83;48,50}^{\text{Hy}}$  are predicted in our output. The two additional contact regions, identified in the partition function, exhibit a significantly lower probability. An additional hairpin over  $R[72, 89]$  is predicted in *fhIA*, instead of the unpaired segment occurring in the natural structure, can be understood in the context of minimizing free energy. Comparing the prediction based on the MSAs (Fig. 6, middle) with the one based on the consensus sequence (Fig. 6, bottom), we observe:

- (1) the secondary structure of *fhIA* agrees better with the annotation joint structure (Fig. 6, top),
- (2) the leftmost hybrid agrees better with that of the annotated structure.
- (3) the binding-site probability (see SM, Section 5, eq. (5.5)) of the leftmost hybrid increases by nearly 40%.

On the flip side, due to the gaps in seven out of eight subsequences induced by  $R[98, 102]$  (Column 98-102 in *fhIA*), the prediction quality of the right-most hybrid and its corresponding contact-region probability decreases slightly.

Let us next contrast our results with those of `PETcofold`, see Fig. 7. The latter predicts *one* of the two interaction sites. The second site is predicted subject to the condition that constrained stems were not extended (Seemann *et al.*, 2010). It can furthermore be observed that in order to predict the second hybrid, at the same time the secondary structures prediction of both *fhIA* and *OxyS* gets worse. `ripalign` predicts both: the interaction sites situated in *fhIA* and comes close to predicting the secondary structures of *fhIA* as well as *OxyS* without any additional constraints.

	I	II	III
1	$J_{37,40;79,82}^{\text{Hy}}$	$J_{40,41;50,51}^{\text{Hy}}$	$J_{5,6;9,10}^{\text{Hy}}$
2	$J_{40,41;50,51}^{\text{Hy}}$	$J_{39,40;51,52}^{\text{Hy}}$	$J_{76,78;90,92}^{\text{Hy}}$
3	$J_{76,78;90,92}^{\text{Hy}}$	$J_{76,78;90,92}^{\text{Hy}}$	$J_{37,40;79,82}^{\text{Hy}}$
4	$\mathbf{R}_{11} \mathbf{S}_{10}$	$J_{11,12;9,10}^{\text{Hy}}$	$J_{78,80;89,91}^{\text{Hy}}$
5	$J_{16,18;33,35}^{\text{Hy}}$	$J_{78,80;89,91}^{\text{Hy}}$	$J_{11,12;51,52}^{\text{Hy}}$
6	$J_{54,57;65,68}^{\text{Hy}}$	$J_{54,57;65,68}^{\text{Hy}}$	$J_{16,17;47,48}^{\text{Hy}}$

**Table 2. Top 6 probable hybrids predicted by `rip` and `ripalign`:** Interaction of two specific RNA molecules, *SLI* and *SmY-10* of *Caenorhabditis elegans* as illustrated in Fig. 8. The top 6 probable hybrids predicted by `rip` implemented by Huang *et al.* (2010) is shown in column I. The hybrids listed in column II are predicted by `ripalign` without any structure constraint. The hybrids listed in Column III are predicted by `ripalign` under the structural constraints that 5'-AAUUUUUG-3' ( $R[56, 62]$ ) and 3'-GUUUAA-5' ( $S[25, 31]$ ) are Sm-binding sites (colored in red) in *SmY-10* and *SL-1*, respectively. Here, we use  $J_{i,j;h,l}^{\text{Hy}}$  to denote the hybrid induced by  $R[i, j]$  and  $S[h, l]$ .

#### (b): The *SmY-10/SL-1* interaction of *C. elegans*

MacMorris *et al.* (2007) stipulated that *SmY-10* RNA, possible involved in *trans*-splicing, interacts with the splice leader RNA (*SLI* RNA). In Fig. 8, we show that the Sm-binding sites (colored in red) of the RNA molecules *SmY-10* and *SL-1* are  $R[56, 62]$  and  $S[25, 31]$ , respectively. In Fig. 8, the top structure is being predicted by `rip` (Huang *et al.*, 2010). We observe that firstly a stack in *SmY-10* consisting of the single arc  $R_{24}S_{67}$  and secondly the nucleotides of the Sm-binding sites form intra base pairs. The canonical grammar presented here restricts the configuration ensemble to canonical joint structures, resulting in the structure presented in Fig. 8 (middle) in which the peculiar isolated interaction arc disappears. However, the nucleotides of the Sm-binding sites still form either intra or inter-molecular base pairs. Incorporating the structural constraints option we derive the bottom structure displayed in Fig. 8. Here the Sm-binding sites are single-stranded. In Table. 3 we elaborate this point further and show that the combination of canonical grammar and structural constraints eliminate unwanted hybrids and “free” the nucleotides attributed to Sm-binding sites of unwanted interactions.

#### (c): The *U4/U6* interaction

Two of the snRNAs involved in pre-mRNA splicing, *U4* and *U6*, are known to interact by base pairing (Zucker-Aprison *et al.*, 1988). We divided all known metazoan *U4* and *U6* snRNAs into three distinct groups and alignments: protostomia without insects, insects and deuterostomia (Marz *et al.*, 2008). Marz *et al.* (2008) observed that insects behave in their secondary structure different from other protostomes, see Fig. 9. Comparing all the predicted *U4/U6* interactions, displayed in Fig. 9, we can conclude:

- (1) the secondary partial structures of the *U4/U6* complex for all three groups predicted by `ripalign` agree predominantly with the described secondary structures in metazoans (Thomas *et al.*, 1990; Otake *et al.*, 2002; Shambaugh *et al.*, 1994; López *et al.*, 2008; Shukla *et al.*, 2002), e.g. as depicted in Fig. 9 (top) for *C. elegans* (Zucker-Aprison *et al.*, 1988).
- (2) for all three groups, Stem I and II (Fig. 9, top) are highly conserved. External ascendancies, such as protein interactions may stabilize stem II additionally.
- (3) for all three groups, the 5' hairpin of *U4* snRNA seems highly conserved to interact with the *U6* snRNA. This RNA feature is not fully understood, since this element is also believed to contain intraloop interactions and may bind to a 15.5kDa protein Vidovic *et al.* (2000).
- (4) for all metazoans, the *U6* snRNA shows conserved intramolecular interactions between the 3' part and the region downstream of the 5'-hairpin.
- (5) for deuterostomes (Fig. 9, bottom), with a contact-region probability of 45.5%, our algorithm identifies a third *U4/U6* interaction, Stem III, to be conserved, which agrees with the findings in Jakab *et al.* (1997);

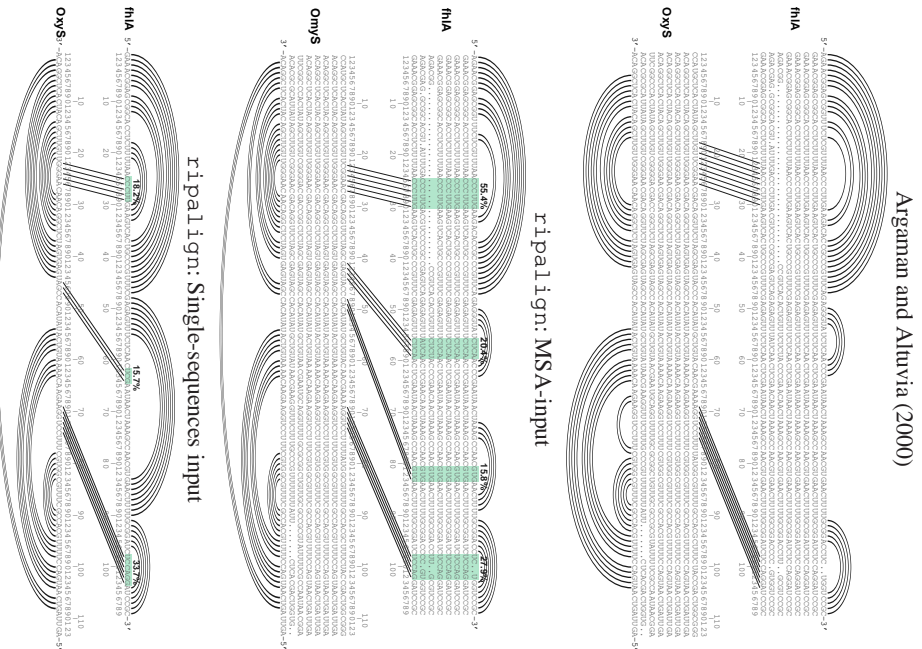


**Fig. 6. Improvement of prediction via incorporating evolutionary history.** Top: the annotated structure of the *hflA/OxyS* interaction Argaman and Aluivia (2000); Middle: the joint structure predicted by *ripalign* with MSAs as input; Bottom: the joint structure predicted by *ripalign* with the consensus sequences of MSAs as input. The target site (green boxes) probabilities (defined in SM Section. 5, eq. (5.5)) computed by *ripalign* are annotated explicitly if  $> 10\%$  or just by  $\leq 10\%$ , otherwise. For instance, the probability of the left-most contact region  $R_{[25, 30]}$  in *hflA* (middle) is 55.4%.

Brow and Vidaver (1995). For protozoans, a similar feature with a contact region probability of  $\leq 10\%$  can also be assumed.

(6) for both: protozoemia (without insects) and deuterozoans, the 5' hairpin of *U6* snRNA seems to interact with the *U4* 3' hairpin. However, this observation does not hold for insects, which agrees with a systematically different secondary structure of spliceosomal RNAs in insects (Marz *et al.*, 2008).

We finally remark that the quality of prediction of *ripalign* depends critically on the quality of the MSAs. This issue of alignment quality is not easily solved: creating an alignment without knowing the structure is unlikely to produce a structural alignment. It might be an option to realign the sequences of an RNA family taking both the predicted secondary structures and predicted joint structure with other RNA families into consideration. Furthermore, *ripalign* is limited by its *a priori* output class of joint structures. Thus *ripalign* cannot identify any joint structures exhibiting pseudoknots. To save computational resources, we

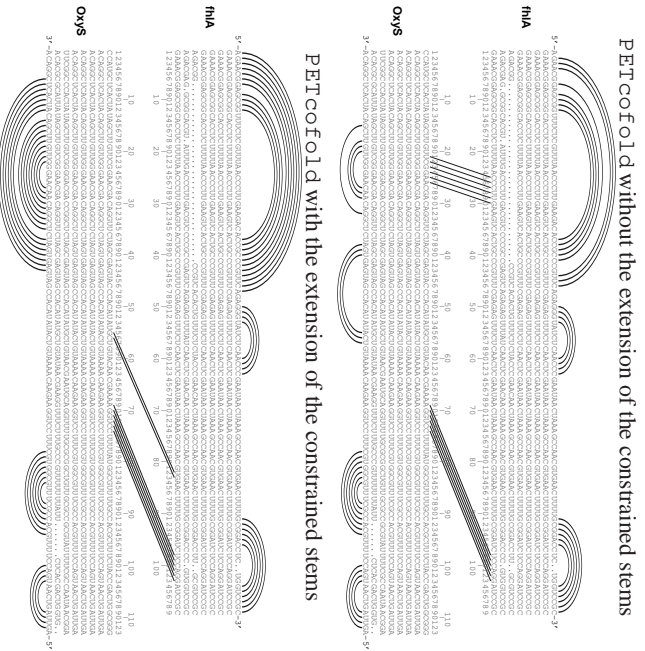


**Fig. 7. The joint structures of *hflA/OxyS* predicted by PETcofold:** The prediction was performed (top) without and (bottom) with the extension of the constrained stems based on the same MSAs showed in Fig. 6. Here, the extension of constrained stems is a specific programming-technique of Seemann *et al.* (2010) to avoid incomplete stems appear in their prediction result.

stipulate that only alignment positions contribute as indices and loop sizes. The assumption may cause, for instance, the existence of some interior arcs  $R_i R_j$  having arc-length smaller than three. Bernhart *et al.* (2008) showed that this problem can be improved substantially by introducing a different, more rational handling of alignment gaps, and by replacing the rather simplistic model of covariance scoring with more sophisticated RIBOSUM-like scoring matrices.

**Acknowledgements.** We want to thank Fenix W.D. Huang and Jan Engelhardt for helpful suggestions. We thank Sharon Selzso of the Modular and BICoC Benchmark Center, IBM and Kathy Tzeng of IBM Life Sciences Solutions Enablement. Their support was vital for all computations presented here. We thank Albrecht Bindererif, Elizabeth Chester and Stephen Rader for their *U4/U6* analysis. This work was supported by the 973 Project of the Ministry of Science and Technology, the PCSIRT Project of the Ministry of Education, and the National Science Foundation of China to CMR and his lab, grant No. STA 850/7-1 of the Deutsche Forschungsgemeinschaft under the auspices of SPP-1258 “Small Regulatory RNAs in Prokaryotes”, as well as the European Community FP-6 project SYNLET (Contract Number 043312) to Peter F. Stadler and his lab.

## REFERENCES

- Akutsu, T. (2000) Dynamic programming algorithms for RNA secondary structure prediction with pseudoknots. *Disc. Appl. Math.*, **104**, 45–62.
- Alkan, C., Karakoc, E., Nadeau, J., Sahinalp, S. and Zhang, K. (2006) RNA-RNA interaction prediction and antisense RNA target search. *J. Comput. Biol.*, **13**, 267–282.
- Antbos, V. (2004) The functions of animal microRNAs. *Nature*, **431**, 350–355.
- Andronescu, M., Zhang, Z. C. and Condon, A. (2005) Secondary structure prediction of interacting RNA molecules. *J. Mol. Biol.*, **345**, 1101–1112.

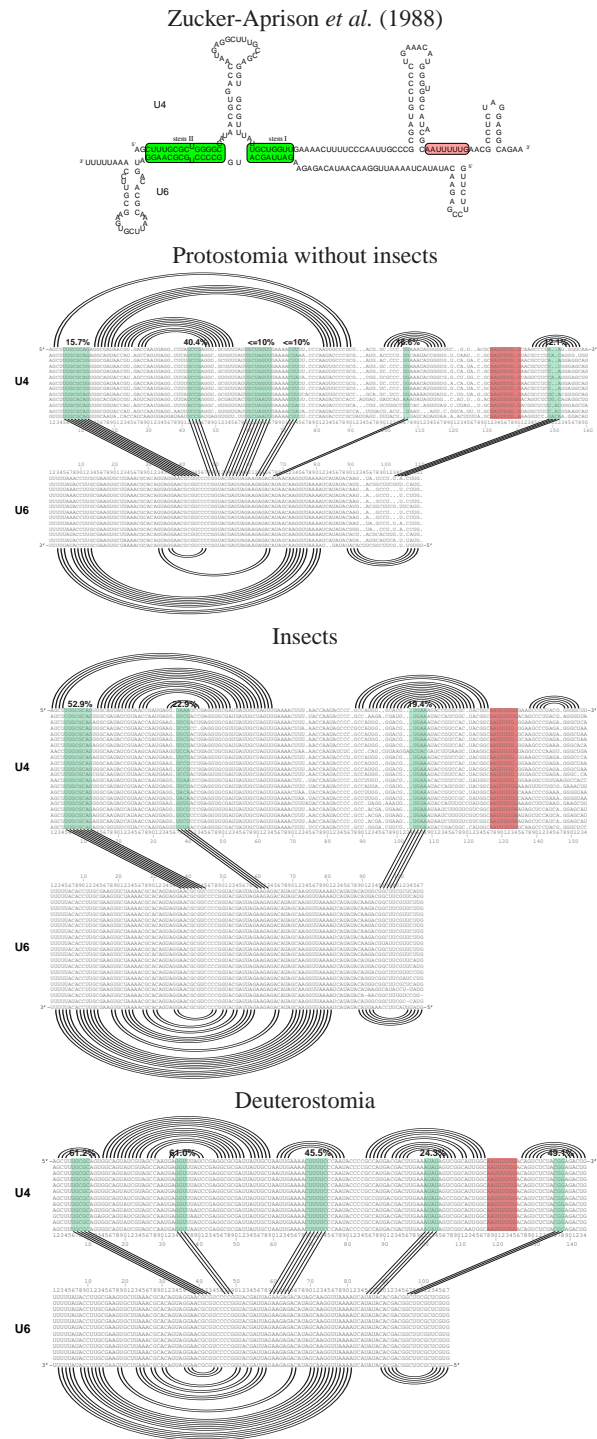
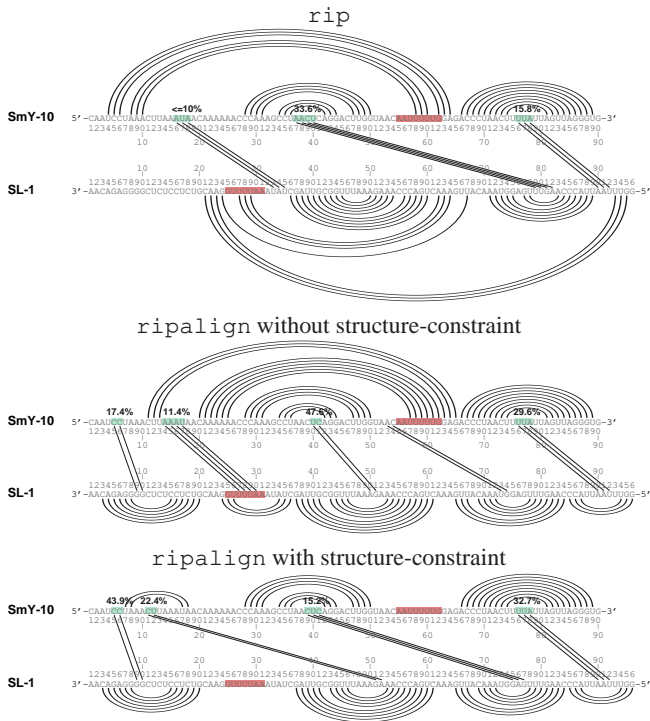


**Fig. 8. ripalign versus rip:** Interaction of two specific RNA molecules, *SL1* and *SmY-10* of *Caenorhabditis elegans*. The Sm-binding sites (colored in red) in the RNA molecules *SmY-10* and *SL-1* are 5'-AAUUUUUG-3'(R[56, 62]) and 3'-GUUUUAA-5'(S[25, 31]), respectively. The joint structure contain a single interior arc  $R_{24}S_{67}$ (top) is predicted by rip implemented by Huang *et al.* (2010). The joint structure (middle) is predicted by ripalign without any structural constraint. The joint structure (bottom) is predicted by ripalign under the structural constraints that 5'-AAUUUUUG-3'(R[56, 62]) and 3'-GUUUUAA-5'(S[25, 31]) are Sm-binding sites in the RNA molecules *SmY-10* and *SL-1*, respectively. The target site (green boxes) probabilities computed by ripalign are annotated explicitly if > 10% or just by  $\leq 10\%$ , otherwise.

Argaman, L. and Altuvia, S. (2000) *fhlA* repression by *OxyS* RNA: kissing complex formation at two sites results in a stable antisense-target RNA complex. *J. Mol. Biol.*, **300**, 1101–1112.

Bachelier, J., Cavaill, J. and Huttenhofer, A. (2002) The expanding snoRNA world. *Biochimie*, **84**, 775–779.

Bernhart, S., Hofacker, I., Will, S., Gruber, A. and Stadler, P. (2008) RNAalifold: improved consensus structure prediction for RNA alignments. *BMC Bioinformatics*, **9**, 474–487.

Bernhart, S., Tafer, H., Mückstein, U., Flamm, C., Stadler, P. and Hofacker, I. (2006) Partition function and base pairing probabilities of RNA heterodimers. *Algorithms Mol. Biol.*, **1**, 3.

Brow, D. and Vidaver, R. (1995) An element in human U6 RNA destabilizes the U4/U6 spliceosomal RNA complex. *RNA*, **1**, 122–131.

Brunel, C., Marquet, R., Romby, P. and Ehresmann, C. (2003) RNA loop-loop interactions as dynamic functional motifs. *Biochimie*, **84**, 925–944.

Busch, A., Richter, A. S. and Backofen, R. (2008) IntaRNA: efficient prediction of bacterial sRNA targets incorporating target site accessibility and seed regions. *Bioinformatics*, **24**, 2849–2856.

Chitsaz, H., Backofen, R. and Sahinalp, S. C. (2009a) biRNA: Fast RNA-RNA binding sites prediction. In *Proceedings of the 9th Workshop on Algorithms in Bioinformatics (WABI)*, volume 5724 of *LNCS*, pp. 25–36. Springer, Berlin / Heidelberg.

**Fig. 9. The U4-U6 interaction prediction with Sm-binding site constraint in U4.** The Sm-binding site in molecule *U4* is 5'-AAUUUUUG-3'(colored in red). Top of the figure is the natural structure of *U4/U6* of *C. elegans* depicted by Zucker-Aprison *et al.* (1988), in which the stem I, stem II and Sm-binding site are colored in green and red, respectively. The joint structures of protostomia (without insects), insects and deuterostomia (from top to bottom) are predicted by ripalign under the Sm-binding site constraint. The target site (green boxes) probabilities computed by ripalign are annotated explicitly if > 10% or just by  $\leq 10\%$ , otherwise.

- Chitsaz, H., Salari, R., Sahinalp, S. C. and Backofen, R. (2009b) A partition function algorithm for interacting nucleic acid strands. *Bioinformatics*, **25**, i365–i373.
- Ding, Y. and Lawrence, C. E. (2003) A statistical sampling algorithm for RNA secondary structure prediction. *Nucleic Acid Res.*, **31**, 7280–7301.
- Forne, T., Labourier, E., Antoine, E., Rossi, F., Gallouzi, I., Cathala, G., Tazi, J. and Brunel, C. (1996) Structural features of U6 snRNA and dynamic interactions with other spliceosomal components leading to pre-mRNA splicing. *Biochimie*, **78**, 434–442.
- Gaspin, C. and Westhof, E. (1995) An interactive framework for RNA secondary structure prediction with a dynamical treatment of constraints. *J. Mol. Biol.*, **254**.
- Geissmann, T. and Touati, D. (2004) Hfq, a new chaperoning role: binding to messenger RNA determines access for small RNA regulator. *EMBO J.*, **23**, 396–405.
- Hershberg, R., Altuvia, S. and Margalit, H. (2003) A survey of small RNA-encoding genes in *Escherichia coli*. *Nucleic Acids Res.*, **31**, 1813–1820.
- Hofacker, I., Fekete, M. and Stadler, P. (2002) Secondary structure prediction for aligned RNA sequences. *J. Mol. Biol.*, **319**, 1059–1066.
- Hofacker, I. L., Fontana, W., Stadler, P. F., Bonhoeffer, L. S., Tacker, M. and Schuster, P. (1994) Fast folding and comparison of RNA secondary structures. *Monatsh. Chem.*, **125**, 167–188.
- Huang, F., Qin, J., Reidys, C. and Stadler, P. (2010) Target prediction and a statistical sampling algorithm for RNA-RNA interaction. *Bioinformatics*, **26**, 175–181.
- Huang, F. W. D., Qin, J., Stadler, P. F. and Reidys, C. M. (2009) Partition function and base pairing probabilities for RNA-RNA interaction prediction. *Bioinformatics*, **25**, 2646–2654.
- Jabbari, H., Condon, A., Pop, A., Pop, C. and Zhao, Y. (2007) Hfold: RNA pseudoknotted secondary structure prediction using hierarchical folding. In R., G. (ed.), *In algorithms in Bioinformatics, 7th international workshop, WABI 2007*. Philadelphia, PA, USA.
- Jakab, G., Mougou, A., Kis, M., Pollák, T., Antal, M., Branlant, C. and Solymosy, F. (1997) *Chlamydomonas* U2, U4 and U6 snRNAs. An evolutionary conserved putative third interaction between U4 and U6 snRNAs which has a counterpart in the U4atac-U6atac snRNA duplex. *Biochimie*, **79**, 387–395.
- López, M., Rosenblad, M. and Samuelsson, T. (2008) Computational screen for spliceosomal RNA genes aids in defining the phylogenetic distribution of major and minor spliceosomal components. *Nucleic Acids Res.*, **36**, 3001–3010.
- MacMorris, M., Kumar, M., Lasda, E., Larsen, A., Kraemer, B. and Blumenthal, T. (2007) A novel family of *C. elegans* snRNPs contains proteins associated with *Trans*-splicing. *RNA*, **13**, 511–520.
- Marz, M., Kirsten, T. and Stadler, P. F. (2008) Evolution of spliceosomal snRNA genes in metazoan animals. *J. Mol. Evol.*, **67**, 594–607.
- Mathews, D., Sabina, J., Zuker, M. and Turner, D. H. (1999) Expanded sequence dependence of thermodynamic parameters improves prediction of RNA secondary structure. *J. Mol. Biol.*, **288**, 911–940.
- McCaskill, J. S. (1990) The equilibrium partition function and base pair binding probabilities for RNA secondary structure. *Biopolymers*, **29**, 1105–1119.
- Mneimneh, S. (2009) On the approximation of optimal structures for RNA-RNA interaction. *IEEE/ACM Trans. Comp. Biol. Bioinf.*, **6**, 682–688.
- Mückstein, U., Tafer, H., Bernhard, S. H., Hernandez-Rosales, M., Vogel, J., Stadler, P. F. and Hofacker, I. L. (2008) Translational control by RNA-RNA interaction: Improved computation of RNA-RNA binding thermodynamics. In Elloumi, M., Küng, J., Linial, M., Murphy, R. F., Schneider, K. and Toma, C. T. (eds.), *Bioinformatics Research and Development — BIRD 2008*, volume 13 of *Comm. Comp. Inf. Sci.*, pp. 114–127. Springer, Berlin.
- Mückstein, U., Tafer, H., Hackermüller, J., Bernhard, S. H., Stadler, P. and Hofacker, I. L. (2006) Thermodynamics of RNA-RNA binding. *Bioinformatics*, **22**, 1177–1182.
- Murchison, E. and Hannon, G. (2004) miRNAs on the move: miRNA biogenesis and the RNAi machinery. *Curr. Opin. Cell Biol.*, **16**, 223–229.
- Otake, L., Scamborova, P., Hashimoto, C. and Steitz, J. (2002) The divergent U12-type spliceosome is required for pre-mRNA splicing and is essential for development in *Drosophila*. *Mol. Cell*, **9**, 439–446.
- Pervouchine, D. (2004) IRIS: Intermolecular RNA interaction search. *Proc. Genome Informatics*, **15**, 92–101.
- Rehmsmeier, M., Steffen, P., Höchsmann, M. and Giegerich, R. (2004) Fast and effective prediction of microRNA/target duplexes. *Gene*, **10**, 1507–1517.
- Ren, J., Rastegari, B., Condon, A. and Hoos, H. H. (2005) Hotknots: heuristic prediction of microRNA secondary structures including pseudoknots. *RNA*, **11**, 1494–1504.
- Repoila, F., Majdalani, N. and Gottesman, S. (2003) Small non-coding RNAs, co-ordinators of adaptation processes in *Escherichia coli*: The RpoS paradigm. *Mol. Microbiol.*, **48**, 855–861.
- Rivas, E. and Eddy, S. R. (1999) A dynamic programming algorithms for RNA structure prediction including pseudoknots. *J. Mol. Biol.*, **285**, 2053–2068.
- Salari, R., Backofen, R. and Sahinalp, S. (2009) Fast prediction of RNA-RNA interaction. In *Proceedings of the 9th Workshop on Algorithms in Bioinformatics (WABI)*, volume 5724 of *LNCS*, pp. 261–272. Springer, Berlin / Heidelberg.
- Seemann, S., Gorodkin, J. and Backofen, R. (2008) Unifying evolutionary and thermodynamic information for RNA folding of multiple alignments. *Nucleic Acids Res.*, **36**.
- Seemann, S., Richter, A., Gorodkin, J. and Backofen, R. (2010) Hierarchical folding of multiple sequence alignments for the prediction of structures and RNA-RNA interactions. *Algorithms for Molecular Biology*, **5**. Doi:10.1186/1748-7188-5-22.
- Shambaugh, J., Hannon, G. and Nilsen, T. (1994) The spliceosomal U small nuclear RNAs of *Ascaris lumbricoides*. *Mol. Biochem. Parasitol.*, **64**, 349–352.
- Shukla, G., Cole, A., Dietrich, R. and Padgett, R. (2002) Domains of human U4atac snRNA required for U12-dependent splicing in vivo. *Nucleic Acids Res.*, **30**, 4650–4657.
- Thomas, J., Lea, K., Zucker-Aprison, E. and Blumenthal, T. (1990) The spliceosomal snRNAs of *Caenorhabditis elegans*. *Nucleic Acids Res.*, **18**, 2633–2642.
- Vidovic, I., Nottrott, S., Hartmuth, K., Lüthmann, R. and Ficner, R. (2000) Crystal structure of the spliceosomal 15.5kD protein bound to a U4 snRNA fragment. *Mol. Cell*, **6**, 1331–1342.
- Zucker-Aprison, E., Thomas, J. and Blumenthal, T. (1988) *C. elegans* snRNAs: a model for U4/U6 base pairing. *Nucleic Acids Res.*, **16**, 7188–7188.



